EUSIPCO 2013 1569740579

SPARSE RECONSTRUCTION TECHNIQUES IN TOMOGRAPHIC SAR INVERSION

Xiao Xiang Zhu [1, 2], *Richard Bamler* [1, 2]

(1) Remote Sensing Technology Institute (IMF), German Aerospace Center (DLR), Oberpfaffenhofen, 82234 Wessling, Germany (xiao.zhu@dlr.de)

(2) Chair of Remote Sensing Technology (LMF), Technische Universität München, Arcisstrasse 21, 80333 Munich, Germany

ABSTRACT

Tomographic SAR inversion is essentially a spectral analysis problem. The resolution in the elevation direction depends on the spread of orbit tracks. Since the orbits of modern meter-resolution space-borne SAR systems, such as TerraSAR-X, are tightly controlled, the tomographic elevation resolution is at least an order of magnitude lower than in range and azimuth. Hence, super-resolution reconstruction algorithms are desired. Considering the sparsity of the signal in elevation, here the theory of compressive sensing comes into play. In this paper, recent developments on compressive sensing applied to tomographic SAR inversion are presented: A compressive sensing based algorithm "SL1MMER" was proposed; The ultimate bounds of the technique on localization accuracy and super-resolution power were investigated; the super-resolution capability of SL1MMER is demonstrated using TerraSAR-X real data examples.

Index Terms— compressive sensing, sparsity, SL1MMER algorithm, tomographic SAR inversion

1. INTRODUCTION

A conventional spaceborne or airborne Synthetic Aperture Radar (SAR) maps the three-dimensional (3-D) reflectivity distribution of a scene to be imaged into the 2-D azimuth-range (*x* - *r*) plane. This projection particularly handicaps the interpretation of SAR images of (i) volumetric scatterers and (ii) of urban areas and man-made objects, i.e. objects with constructive elements oriented at steeper angles than the local incidence angle.

SAR Tomography (TomoSAR) is a technique that allows resolving scatterer densities in the third native radar co-ordinate "elevation (*s*)" (also referred to as slant–height, orthogonal to the azimuth-range plane) [1]-[3]. It extends the synthetic aperture principle – as used in the azimuth direction – also to the elevation direction by exploiting multiple passes of the radar at slightly different orbit positions to establish a virtual array of antennas, as depicted in Figure 1. The synthetic aperture in elevation allows real 3D imaging. By stacking all the multiview coherent images and by performing the tomographic processing, *s*-profiles can be retrieved for every *x*-*r* pixel. These profiles may be continuous in the case of forest biomass imaging. In the case of urban mapping, however, most of the *s*-profiles are *sparse*, i.e. they consist only of a few discrete scatterers, typically corresponding to scatterers located on the ground, facade and roof. This article is devoted to the latter application.

The inherent (Rayleigh) elevation resolution ρ_s of the tomographic arrangement is related to the spread Δb of this array by $\rho_s = \lambda r / 2\Delta b$. Since the orbits of modern meter-resolution spaceborne SAR systems, like TerraSAR-X, are tightly controlled, the tomographic elevation resolution is at least an order of magnitude lower than in range and azimuth. The layover phenomenon in a SAR image of an urban area is mainly caused by the following two scenarios: (i) buildings with different heights in layover with the ground or (ii) taller building in layover with the ground and the roof of a lower building. Both scenarios suggest that double scatterer pairs with smaller elevation distances will be more frequent than those with larger distances. Therefore, super-resolution (SR) is crucial for VHR tomographic SAR reconstruction in urban environment. This makes super-resolving TomoSAR algorithms particularly important for urban mapping [4][5].

Considering the aforementioned sparsity of the signal in elevation, here the theory of compressive sensing comes into play [6] [7]. In this paper, an overview on compressive sensing applied to tomographic SAR inversion is presented: A compressive sensing based "SL1MMER" algorithm was proposed; The ultimate bounds of the technique on localization accuracy and super-resolution power were investigated; the super-resolution capability of SL1MMER is demonstrated using TerraSAR-X real data examples.

2. TOMOSAR SYSTEM MODEL

Since the elevation antenna array is in the far-field of the imaged objects, the complex signal received at any of the radar positions b_n is a sample of the Fourier transform of the reflectivity profile in elevation $\gamma(s)$:

$$g_n = \int_{\Delta s} \gamma(s) \exp(-j2\pi\xi_n s)\, ds, \qquad n = 1, \ldots, N \tag{1}$$

where $\xi_n = -2b_n/(\lambda r)$ is the spatial (elevation) frequency. Therefore, retrieval of the *s*-profile is framed as a spectral estimation problem and scatterers showing a good degree of coherence can be identified by looking for the peaks in the focused reflectivity function.

Since the multipass dataset is acquired at different time instants, sometimes over a period of years, possible motion and deformation of objects must be additionally considered in the process of estimation of the *s*-profiles, either as useful information (subsidence, tectonics, landslides, etc.) or simply as nuisance parameters. Space/velocity (4D) imaging techniques (Differential SAR Tomography, D-TomoSAR), which are an extension of 3D imaging, can also be applied to measure the deformation parameters (velocity spectrum) of any temporal coherent scatterer in the focused 3D space [8]-[10]. If motion is considered, eq. (1) is extended to a 2D or even higher dimensional Fourier transform, depending on how many motion modes are accounted for (e.g. linear, periodic, thermal, etc.).

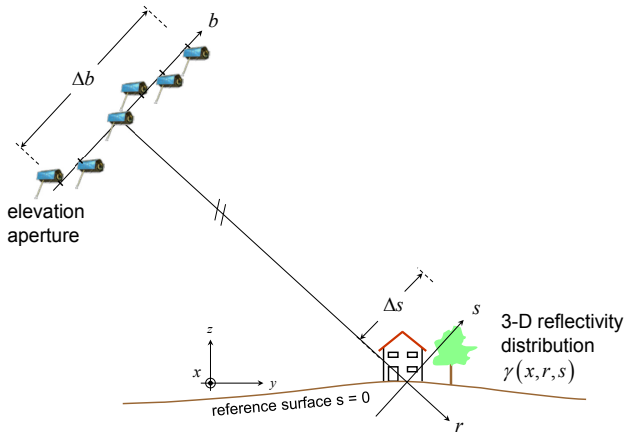

Figure 1: TomoSAR geometry in the range-elevation plane

3. THE SL1MMER ALGORITHM

As mentioned before, the highly anisotropic resolution element renders the signal sparse in elevation, i.e. we expect only a few (K = 1…4) point-like scatterers along elevation. Compressive Sensing (CS), as a favorable sparse reconstruction technique, has been recently introduced to radar [6] [7].

3.1 The SL1MMER algorithm [11]

In presence of noise $\boldsymbol{\varepsilon}$, the discrete TomoSAR system model (1) can be written as:

$$\mathbf{g} = \mathbf{R}\,\boldsymbol{\gamma} + \boldsymbol{\varepsilon} \qquad (2)$$

where $\mathbf{g}$ is the measurement vector with N elements, $\boldsymbol{\gamma}$ is the reflectivity function uniformly sampled in elevation at s_l (l = 1,…,L). $\mathbf{R}$ is an $N\times L$ irregularly sampled discrete Fourier transform mapping matrix and the sampling positions ξ_n are a function of the elevation aperture positions b_n.

The SL1MMER algorithm consists of three main steps: 1) a dimensionality scale-down by L_1 norm minimization, 2) model selection and 3) parameter estimation. Since L>>N, the system model (1) is severely under-determined. As described in [11], $\boldsymbol{\gamma}$ is sparse in the object domain for VHR space-borne X-band TomoSAR and can be reconstructed by:

$$\hat{\boldsymbol{\gamma}} = \arg\min_{\boldsymbol{\gamma}} \left\{ \left\| \mathbf{g} - \mathbf{R}\boldsymbol{\gamma} \right\|_2^2 + \lambda_K \left\| \boldsymbol{\gamma} \right\|_1 \right\} \qquad (3)$$

where λ_K is the Lagrange multiplier. Eq. (3) gives a robust estimate of the plausible positions of the scatterers, among which there might be a few outliers contributed by noise. Model selection is used to clean the $\hat{\boldsymbol{\gamma}}$ estimate of spurious, non-significant scatterers and to finally obtain the most likely number $\hat{K}$ of scatterers inside an azimuth-range cell. As a last refinement, the final complex-valued reflectivity for each scatterer $\hat{\boldsymbol{\gamma}}(\hat{\mathbf{s}})$ is obtained by a least-squares estimation. More detailed description of the SL1MMER algorithm can be found in [11] [12].

3.2 Super-resolution Power

The SL1MMER algorithm has been demonstrated to be an efficient estimator and achieves super-resolution factors of 1.5~25 at the interesting parameter range for TomoSAR (see Figure 2), i.e. N=10~100 and SNR=0~10dB [12]. Note that resolution is defined here as the distance of two scatterers of amplitude ratio a_1/a_2 and phase difference $\Delta\varphi$ that can be distinguished as two individual peaks with a probability of 50% at the given SNR and number N of acquisitions. The results shown in Figure 2 are approximately applicable to nonlinear least-squares estimation as well, and hence, although they are derived experimentally, they can be considered as a fundamental bound for SR of spectral estimators. They are applicable for a uniform distribution, i.e. an unknown, $\Delta\varphi$.

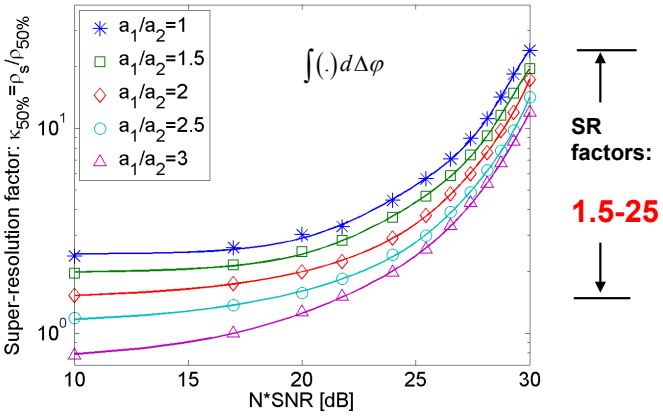

Figure 2: Fundamental bound of super-resolution (SR): SR factor of the SL1MMER algorithm as a function of N SNR under different amplitude ratios a1/a2 of two close scatterers.

4. PRATICAL EXAMPLES

We work with TerraSAR-X high resolution spotlight data with a slant-range resolution of 0.6 m and an azimuth resolution of 1.1 m. The stack used in this paper consists of 30 images covering a time period of more than one year, from February 2008 to June 2009, over downtown Las Vegas. This stack has an elevation aperture size of about 269.5 m, i.e., the inherent elevation resolution is $\rho_s = 40.5$ m, i.e., approximately 20 m resolution in height with the elevation-to-height factor sin θ, where the incidence angle θ is 31.8 degree here.

The Las Vegas Bellagio hotel is chosen as a test building to demonstrate the SR power of SL1MMER since its surrounding infrastructure exhibits strong scatterers that compete with the reflections from the building façade as shown in Fig. 3.a. Two example slices at the positions marked by green arrows in Fig. 3.b are chosen as analysis slices. The reflectivity profiles in the range-elevation plane of the detected double scatterers are extracted using a conventional linear reconstruction method MD [3] [4] (Fig. 4, left) and SL1MMER (Fig. 4, right). Here, the darker color indicates stronger reflection. The different elevation resolution limits of MD and SL1MMER are clearly visible.

Figure 5 presents a 3D view of the Bellagio hotel visualized in GoogleEarth reconstructed by SL1MMER. Compared to PSI, TomoSAR offers in general a tremendous improvement in detailed reconstruction and monitoring of urban areas. Experiments using TerraSAR-X high resolution spotlight data stacks show the scatterer density to be in the order of 600,000~1,000,000/km^2 compared to a PS density in the order of 40,000~100,000 PS/km^2. In particular, together with its SR power, SL1MMER provides ultimate information one can retrieve from the data stack.

Due to the side-looking geometry of SAR, a single stack of SAR images only provides information on one side of a building, i.e. the front or rear side. To serve the function of urban structure monitoring, fusion of the TomoSAR results of multiple stacks from different view angles can provide us with a shadow-free point cloud with high degree of coverage over the entire urban area [13] [14]. At this test site, we have acquired another TerraSAR-X data stack of 30 SAR images from the descending orbit. Figure 6 present the fused 3D point cloud. From Figure 6 detailed city structures can be easily identified. For this test-site, about 35 million scatterers are detected from the two data stacks. Besides its 3D coordinates, each of the points carries additional motion information (velocity of linear and amplitude of seasonal deformation, not displayed here).

5. CONCLUSION & OUTLOOK

In this paper, we have presented an overview on our current progress of compressive sensing applied to tomographic SAR inversion. Taking advantage of the sparse property of the elevation signals, promising super-resolution factors (1.5~25 under the typical parameter range of SAR, i.e. N=10~100, SNR=0~10dB) are achieved with the proposed compressive sensing based SL1MMER algorithm. Practical examples with TerraSAR-X data stacks are presented to demonstrate the super-resolution capability of the algorithm. 3D view of the whole city area reconstructed using two stacks of TerraSAR-X images is shown.

Considering the fact that the information contained in neighboring pixels is correlated, further development will be focused on the exploitation of group sparsity by means of distributed compressive sensing.

REFERENCES

[1] A. Reigber and A. Moreira, “First demonstration of airborne SAR tomography using multibaseline L-band data”, *IEEE Trans. Geosci. Remote Sens.*38 (5), pp. 2142–2152, 2000.

[2] G. Fornaro, F. Serafino, and F. Soldovieri, “Three-dimensional focusing with multipass SAR data”, *IEEE Trans. Geosci. Remote Sens.*, vol. 41, no. 3, pp. 507–517, Mar. 2003.

[3] X. Zhu and R. Bamler,”Very High Resolution Spaceborne SAR Tomography in Urban Environment,“ *IEEE Trans. Geosci. Remote Sens.*, vol. 48, no. 12, pp. 4296–4308, Dec. 2010.

[4] X. Zhu, R. Bamler, “Demonstration of Super-resolution for Tomographic SAR Imaging in Urban Environment,” *IEEE Trans. Geosci. Remote Sens.,* 50 (8), pp.3150-3157, 2012.

[5] L. Roessing, J. Ender, "Multi-Antenna SAR Tomography Using Super Resolution Techniques", proceedings of EUSAR 2000, Munich. pp. 55 - 58, 2000

[6] A. Budillon, A. Evangelista, G. Schirinzi, SAR Tomography from sparse samples. *Proceedings of the IEEE IGARSS*, Cape Town, Africa, 2009.

[7] X. Zhu and R. Bamler, “Very high resolution SAR tomography via compressive sensing”, Proc. ESA FRINGE Workshop, Franscatti, Italy, 2009.

[8] F. Lombardini, “Differential tomography: A new framework for SAR interferometry,” *IEEE Trans. Geosci. Remote Sens.*, vol. 43, no. 1, pp. 37–44, Jan. 2005.

[9] G. Fornaro, D. Reale, and F. Serafino, “Four-dimensional SAR imaging for height estimation and monitoring of single and double scatterers”, *IEEE Trans. Geosci. Remote Sens.,* vol. 47, no. 1, pp. 224–237, Jan. 2009.

[10] X. Zhu, and R. Bamler, “Let’s Do the Time Warp: Multicomponent Nonlinear Motion Estimation in Differential SAR Tomography, ” *IEEE Geosci. Remote Sens. Lett.*8 (4), pp.735-739, 2011.

[11] X. Zhu, R. Bamler, Tomographic SAR Inversion by L1 Norm Regularization – The Compressive Sensing Approach, *IEEE Trans. Geosci. Remote Sens.*, 48 (10), pp. 3839-3846, 2010.

[12] X. Zhu, R. Bamler, “Super-Resolution Power and Robustness of Compressive Sensing for Spectral Estimation with Application to Spaceborne Tomographic SAR,” *IEEE Trans. Geosci. Remote Sens.*, 50(1), pp.247-258, 2012.

[13] S. Gernhardt, X. Cong, M. Eineder, S. Hinz, & R. Bamler, Geometrical Fusion of Multitrack PS Point Clouds, *IEEE Geosci. Remote Sens. Lett.* 9 (1), pp. 38-42, 2012

[14] Y. Wang, X. Zhu, Y. Shi., R. Bamler, “Operational TomoSAR Processing Using TerraSAR-X High Resolution Spotlight Stacks from Multiple View Angles”, *Proceedings of the IEEE IGARSS*, Munich, Germany, 2012.

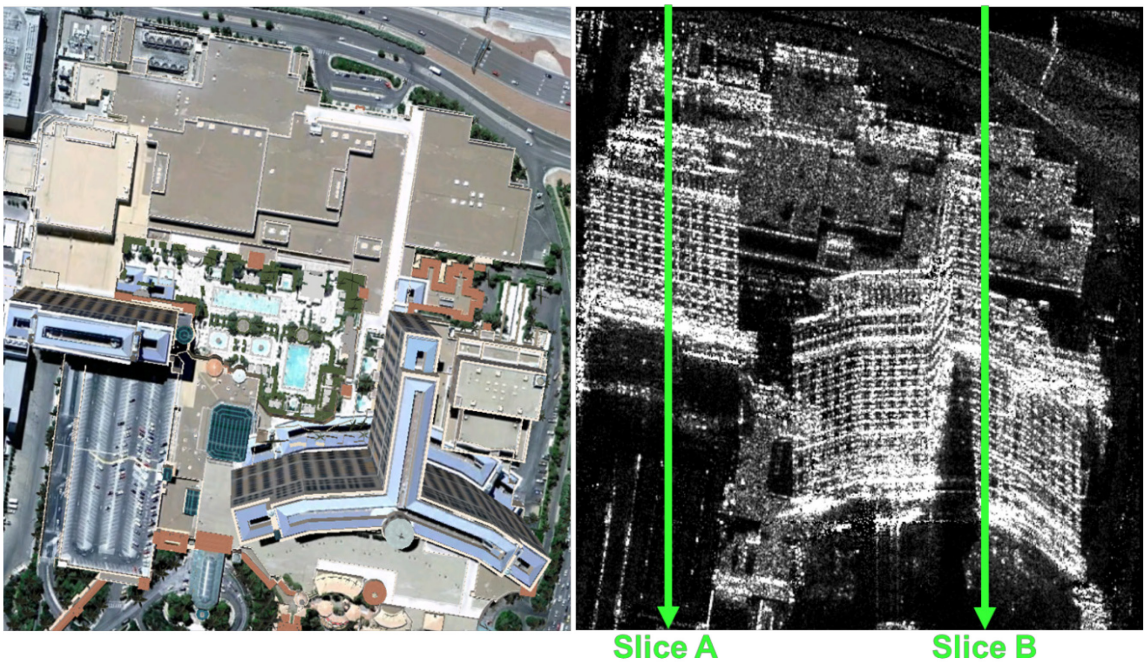

(a) (b)

Figure 3: Test building: Bellagio hotel. (a) Optical image (Copyright Google). (b) TerraSAR-X mean intensity map and the green arrows mark the analysis slice A and B shown in Fig. 4.

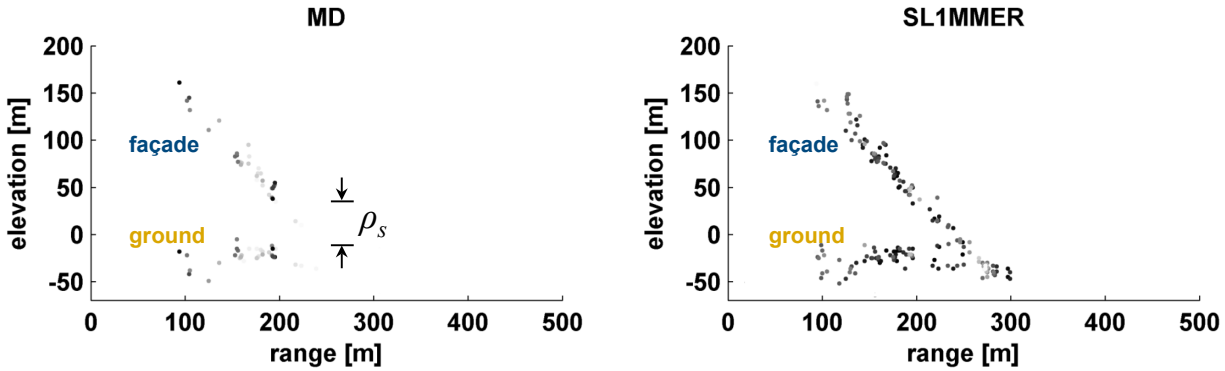

(a) Slice A

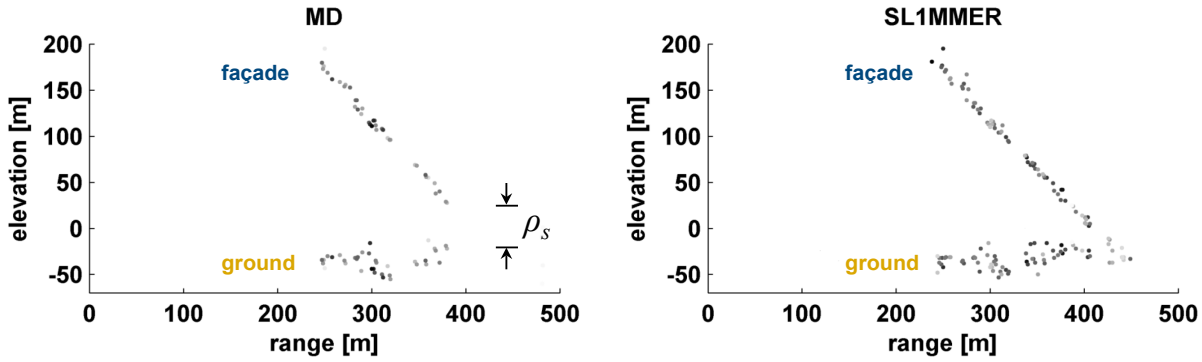

(b) Slice B

Figure 4: (Left) MD versus (right) SL1MMER. Reflectivity profiles of the detected double scatterers for slice A and slice B from Fig. 3. The darker the point the stronger the reflection. Note that there is no flat surface in front of the building. (a) Slice A. (b) Slice B.

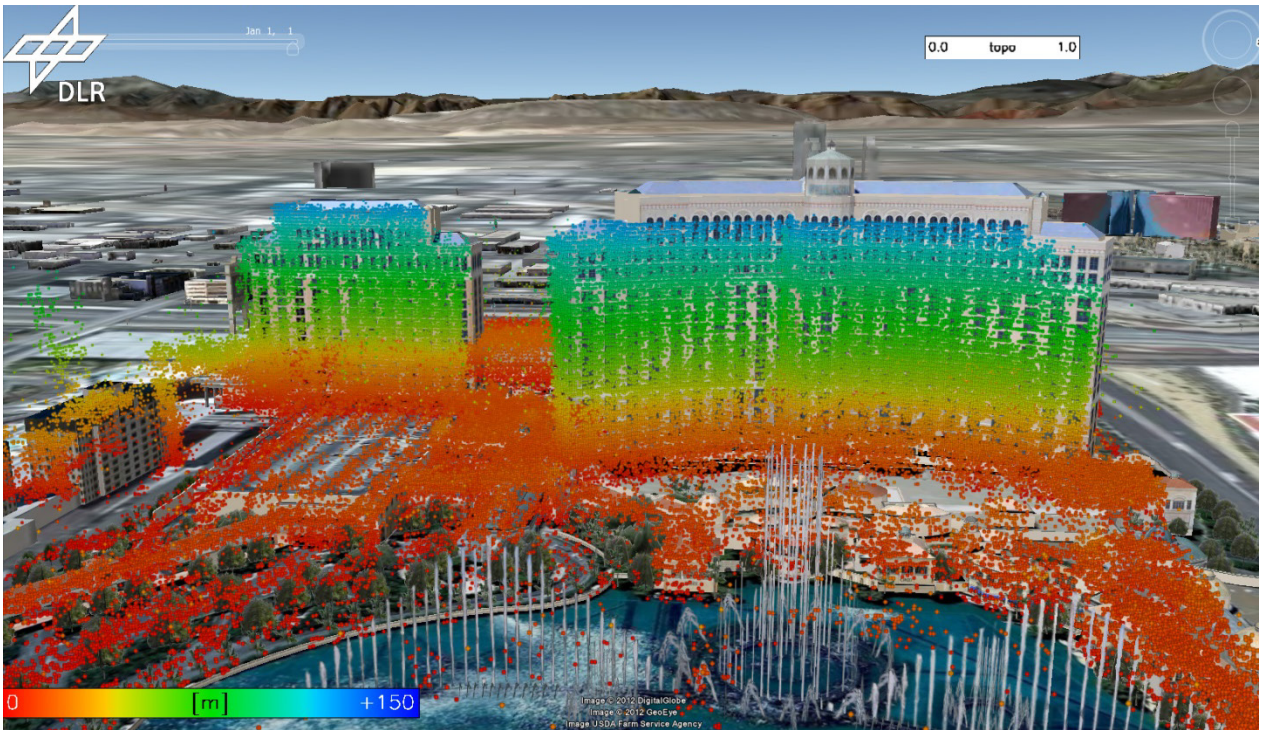

Figure 5: 3D view of the single building visualized in GoogleEarth reconstructed by SL1MMER using a stack of 25 TerraSAR-X images (the color represents height).

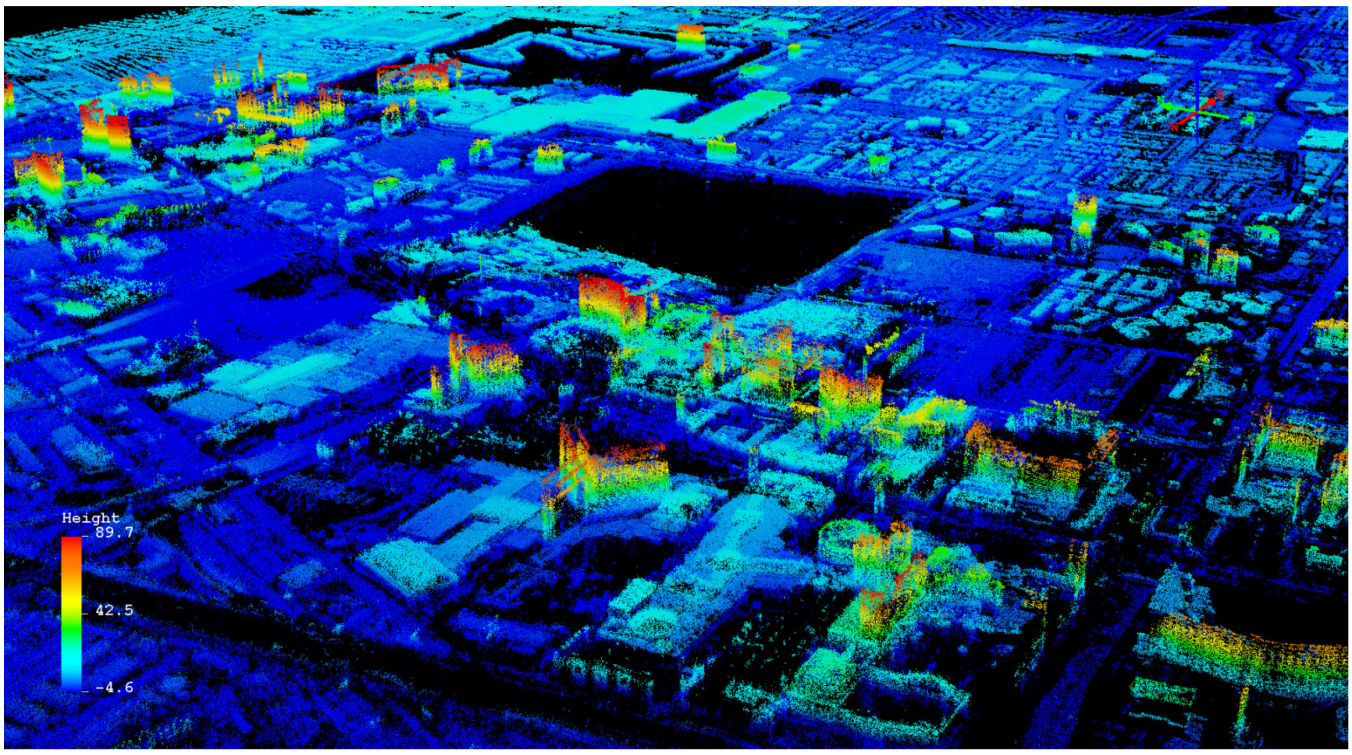

Figure 6: Fusion of two point clouds generated from TerraSAR-X data stacks of ascending and descending orbit. The color represents height.